AJBAR Vol. 3(5), October 2024: 1-15, ISSN: 2811-2881

Arid Zone Journal of Basic and Applied Research

Faculty of Science, Borno State University
Maiduguri, Nigeria

Journal homepage: https://www.azjournalbar.com

Research Article

Adsorption of Methylene Blue onto Composite Activated Carbon derived from Neem Leaves and Moringa Seed Husk

M. A. Zarami[1], A. L Yaumi[1], M. M. Aji[1*], S. Kiman[1], H. Umar[1] and B. Tijjani[2]

[1]Department of Chemical Engineering, University of Maiduguri, Borno State, Nigeria

[2]Department of Chemical Engineering, Federal University of Technology Owerri, Imo State

*Corresponding author's Email: moduajim@unimaid.edu.ng, doi.org/10.55639/607.02010007

ARTICLE INFO:

Keywords:
Neem Leave,
Moringa Seed Husk,
Methylene Blue,
Adsorption

ABSTRACT

This study developed a composite material from Neem Leaves (NL) and Moringa Seed Husk (MSH) for the adsorption of Methylene Blue (MB) dye effluent. The MSH and NL were pyrolyzed at 400°C to synthesize MSH and NL biochar. The biochar was further treated with sodium hydroxide (NaOH) and potassium hydroxide (KOH) as activating agents, separately. The precursors were characterized using Fourier Transform Infrared (FTIR) analysis, Energy Dispersive X-ray Spectroscopy (EDS), and Scanning Electron Microscopy (SEM). SEM analysis revealed transformations in the surface morphology of the material. EDS analysis showed variations in the elemental composition of the materials before and after adsorption of MB dye. FTIR analysis identified the functional groups involved in MB dye removal. Response Surface Methodology (RSM) was performed to determine the optimum operating conditions and to optimize the adsorption capacity. Factors affecting adsorption, including pH, contact time, temperature, concentration, and dosage, were investigated. The produced activated carbon was tested to determine its adsorptive capacity and efficiency using MB dye.It was observed that KOH-impregnated activated carbon exhibited better results than NaOH. KOH, as an activating agent, produced a more porous structure with a higher surface area and better-developed surface functional groups compared to NaOH. This enhanced both physical adsorption and chemical interactions, making KOH-activated carbon more effective in adsorbing MB dye. The surface of KOH-activated carbon was found to be more hydrophilic, facilitating the adsorption of MB from aqueous solutions. Hydrophilic surfaces tend to interact better with aqueous environments, improving the accessibility of the dye to adsorption sites. The best results were achieved at an MB concentration of 400 mg/L, using 0.7 g of residue at a stirring rate of 250 rpm for one hour, with an adsorption efficiency of up to 95%. The adsorption equilibrium and kinetics of MB dye on the activated carbon were examined at 30°C. Adsorption isotherms were determined and correlated with common isotherm equations. The equilibrium data for MB adsorption fit well with the Langmuir model, indicating monolayer coverage of the adsorbate over a homogeneous adsorbent surface. Kinetic studies showed that the adsorption of MB onto NL and MSH-activated carbon fit the pseudo-second-order model, implying that the rate-limiting step is chemisorption.

Corresponding author: M. M. Aji, **Email:** moduajim@unimaid.edu.ng
Department of Chemical Engineering, University of Maiduguri, Borno State, Nigeria

1.0 INTRODUCTION

Dyes are widely used in textiles, rubber, plastics, cosmetics, and many other industries to color products. As a result, they generate large amounts of colored wastewater. Over 10,000 commercially available dyestuffs are produced annually, and it is estimated that 2% of these dyestuffs are discharged into wastewater from related industries. Among various industries, the textile industry ranks first in the use of dyes for fiber dyeing. The total consumption of dyes in the global textile industry exceeds 107 kg/year, with an estimated 90% ultimately consumed on fabrics. Consequently, the global textile industry discharges 1,000 tons or more of dyes into waste streams annually, often untreated or partially treated, which adversely affects ecosystems and livelihoods (Singla *et al.*, 2017).Dyes are persistent in nature, strongly absorb sunlight, reduce the light intensity available to aquatic plants and phytoplankton, reduce photosynthesis and dissolved oxygen in aquatic ecosystems, and lead to increased Chemical Oxygen Demand (COD) (Sharma *et al.*, 2012). Additionally, dye effluents are highly dispersible, difficult to handle, bulky, hazardous, and composed of harmful organic and inorganic chemicals that are toxic and carcinogenic to the microbiome, humans, and animals.Wastewater from dyeing industries is often darker in color, with lower Biochemical Oxygen Demand (BOD), increased COD, and altered pH, temperature, and turbidity. These changes reduce the light absorption by aquatic plants, inhibiting photosynthesis. According to US Public Health (USPH) standards, the maximum allowable COD limit is 4.0 mg/L, while the maximum allowable BOD content ranges from 100 to 300 mg/L.

Moringa is a well-known tropical plant with numerous medicinal and nutritional benefits. Its nutritional value is due to the presence of mineral elements and phytochemicals, which require analysis (Jami & Ahmad, 2019). Moringa seed husks possess excellent coagulation properties and precipitate organic and mineral particles from solution. Chemical coagulants such as aluminum sulfate (Alum) and ferric sulfate or polymers remove suspended particles in water by forming flocs, making the particles easier to filter. Moringa oleifera seed husks are a natural coagulant containing a cationic protein that can clarify muddy water (Gopalakrishnan *et al.*, 2016).Moringa seed husks contain dimeric cationic proteins that adsorb and neutralize colloidal charges in turbid water, allowing the colloidal particles to aggregate and making suspended particles easier to remove through sedimentation or filtration. This natural material is particularly appealing because it is non-toxic and sustainable.

Neem is often considered a weed in many areas. Its fruits, seeds, leaves, stems, and bark contain various phytochemicals. Neem seed extract, notably containing azadirachtin, was recognized in the 1960s as an insect antifeedant, growth disruptor, and pesticide. The yield of azadirachtin from 2 kg of seeds is approximately 6 grams. In addition to azadirachtin and related limonoids, neem seed oil contains glycerides, polyphenols, nimbolides, triterpenes, and beta-sitosterol. The yellow, bitter oil has a garlic-like odor and contains about 2% limonoids. Neem leaves contain quercetin, catechins, carotene, and vitamin C. Fresh neem is reported to contain a maximum of 59.4% moisture, 22.9% carbohydrates, 7.1% protein, 6.2% fiber, 3.4% minerals, and 1% fats, along with other chemicals (Neem Foundation).

Color is a visible contaminant that becomes undesirable even in small quantities due to its appearance (Tiwari, 2002). Several dyes and their decomposition products are toxic to organisms because they are not easily degradable and cannot usually be removed by conventional wastewater treatment systems (O. S. Bello et al., 2013). Thus, the removal of such colored compounds from wastewater has significant environmental implications, as even trace amounts can be toxic and highly visible (Seow & Lim, 2016).This work utilizes readily available agricultural wastes, Neem leaves, and Moringa seed husks as cost-effective precursors to develop composite activated carbon for the removal of Methylene Blue from dye effluent. The enhanced adsorption in dye removal is attributed to the synergistic adsorption properties of the combination, leveraging Moringa's high surface area and porosity along with Neem’s bioactive compounds. This improves dye removal efficiency through enhanced chemical interactions and surface functionality. These

materials offer diverse chemical functionalities, providing multiple adsorption sites through their varied functional groups. Additionally, this method is sustainable, as both Neem and Moringa are abundant agricultural wastes, making the approach eco-friendly and cost-effective. The combination introduces novel synergistic effects, presenting a new research avenue for enhanced adsorption performance. Furthermore, blending these materials potentially improves surface area and porosity, resulting in superior adsorption capacity compared to using them individually.

The combination of Neem leaves and Moringa seed husks also capitalizes on their distinct physical and chemical properties, such as enhanced surface area, diverse functional groups, and complementary adsorption mechanisms. This results in a more efficient, versatile, and sustainable adsorbent compared to single-component materials.Adsorption techniques were used in this experiment due to their ability to selectively remove contaminants, offering flexibility, cost-effectiveness, and high efficiency. In summary, adsorption's versatility, efficiency, and eco-friendliness make it a favored technique. The efficacy of an adsorbent is evaluated based on its capacity, kinetics, surface properties, and reusability, ensuring its suitability for specific applications.

2.1MATERIALS AND METHOD

2.2 Activated Carbon Preparation

Neem leaves and Moringa Seed Husk were collected from the University Staff's Quarters area. They were repeatedly washed with distilled water to remove soluble impurities and particles, then dried in the shade at room temperature for 48 hours. The materials were then placed in a drying oven for 24 hours at a temperature of 105°C. Once dried, the materials were powdered and sieved using a 1 mm mesh before being stored in airtight containers. Subsequently, 100 g of each precursor was separately loaded into a modified muffle furnace with a nitrogen gas flow of 70 ml/min. The materials were heated to a carbonization temperature of 400°C at a heating rate of about 10°C/min. They were kept at the final temperature of 400°C for one hour and then cooled in an inert atmosphere. Response Surface Methodology (RSM) was used to design the experimental runs in order to determine the optimum conditions for both precursors.The samples were impregnated with potassium hydroxide (KOH) and sodium hydroxide (NaOH) based on the results obtained from RSM. They were then left to soak for 24 hours in a covered 250 ml conical flask. The mixture was shaken in a mechanical shaker at 250 rpm for one hour to ensure thorough mixing and allowed to settle. It was shaken again and filtered using Whatman's filter paper (No. 42). The chemically activated carbon was extensively washed with distilled water until the pH of the wash water became neutral. Finally, the chemically activated carbon was dried at 70°C for two hours.

2.3 Characterization of the Adsorbent

Different methods of characterization were used to identify the specific feature that contributed to the enhancement of adsorption capacity of the prepared adsorbent. These include surface functional groups on the adsorbent by using FTIR, surface morphology using Scanning Electron Microscopy (SEM), and elemental chemical composition using Energy Dispersive X-ray Analysis (EDX).

In this experiment, specific parameter ranges—such as pH, contact time, and temperature—are selected based on practical relevance, system behavior, and prior research findings**.** Practical relevance is considered by choosing ranges like pH 6–8, which reflect typical environmental conditions, ensuring the results are applicable to real-world scenarios. Similarly, the chosen contact time and temperature match operational conditions found in industrial and environmental processes. Behavioral sensitivity to pH is also a factor, as extreme values could disrupt adsorbent functionality, so the pH range of 6–8 captures optimal performance without compromising the system. The parameters also ensure stability and consistency, as some adsorbents remain stable only within specific ranges, preserving the integrity of both the adsorbent and adsorbate throughout the experiment. Avoiding extremes in pH or temperature prevents undesirable reactions, such as adsorbent degradation or slow adsorption kinetics. Focusing on optimization, narrowing the range to pH 6–8 allows researchers to fine-tune adsorption performance efficiently. Furthermore, precedents from literature guide the selected ranges, ensuring

comparability with previous studies and conserving resources. Overall, the chosen parameter ranges ensure stability, relevance, and Batch adsorption studies was carried out using 100ppm as initial dye concentration and adsorbent at different dosages (0.1g-1.0g) for both precursors and the activating agents as proposed by RSM and the weighed samples were taken into 250 ml conical flask with 50ml of distilled water. The adsorption capacity was measured for each of the experiment using the UV- spectrophotometer at 663nm. The adsorption capacity of the adsorbent was evaluated by series of adsorption on methylene blue Dye. The adsorption studies were carried out to study the effect of dosage ranging from (0.1-1.0 g); adsorption temperature (30-50 ºC); effect of pH (6-8); effect of time (20-160 min); effect of initial concentration (100 - 500 mg/L). The adsorption Isotherms were evaluated by fitting them to Langmuir, Freundlich and Temkin isotherms model. The kinetics was also studied to ascertain the rate order and nature of the adsorption process.

optimal performance while minimizing unnecessary complexity.

2.4 Batch Adsorption Experiment

The amount of adsorption at equilibrium was obtained using equation (2.1)

$$q_t = \frac{(C_o - C_e)V}{w} \qquad (2.1)$$

Where: q_t adsorption capacity (mg/g) at time t, C_o initial concentration (mg/L), C_e concentration at equilibrium (mg/L), V volume of solution used (mL), w weight of the adsorbent (g).

2.4.1 Adsorption Isotherms

Adsorption isotherms provide information about molecule-surface interactions. They refer to a series of adsorption measurements made at a specific temperature, the results of which are plotted. The adsorption Isotherms and kinetics of the work was determined using Langmuir, Freundlich, Temkin and Pseudo First order, Pseudo Second order models.

$$\frac{C_e}{qe} = \frac{1}{kQ^0} + \frac{C_e}{Q^0} \qquad (2.2)$$

Where Ce is the equilibrium concentration in mg/L Q_0 = maximum adsorption capacity which is the Langmuir constants. K has a unit of L/mg. which is obtained from the slope and the intercept from the plot linear plot.

$$ln\ qe = lnKF + bF\ lnCe \qquad (2.3)$$

Freundlich isotherm is mostly conforms to adsorption of polar substances on molecular sieves and activated carbon. K_F and b_F are the Freundlich constants (Foo & Hameed, 2010).

The Temkin isotherm has been used in the following form:

$$qe = RT/\ b\ lnA + RT\ /b\ lnCe \qquad (2.4)$$

2.4.2 Kinetics Model

Adsorption kinetics mainly studies the reaction rate between adsorbents and adsorbates and the factors affecting the reaction rate. The adsorption data were fitted by kinetic models and the adsorption mechanism was discussed according to the fitting results. The linear forms of the equations are:

$$ln(q_e - q_t) = ln(q_e) - k_1 t \qquad (2.5)$$

Where q_t and q_e are the amounts of metal ions adsorbed (mg/g) at time t, and at equilibrium, respectively, k_1 is the rate constant of pseudo-first-order equation (min^{-1}).

$$\frac{1}{q_e - q_t} = \frac{1}{q_e} + k_2 t \qquad (2.6)$$

Where, q_t and q_e are the amounts of metal ions adsorbed (mg/g) at time t, and at equilibrium, respectively, k_2 is the rate constant of pseudo-second-order equation (g/mg min).

$$q_t = \frac{1}{\beta} ln(\alpha\beta) + \frac{1}{\beta} ln(t) \qquad (2.7)$$

Where, α is the initial adsorption rate (mg/min) and ß is related to the extent of surface coverage and the activated energy for chemisorption (g/mg). A plot of q versus ln (t) gives a linear trace with a slope of (1/ß) and an intercept of 1/ß ln (aß) q_t and q_e are the amounts of methylene blue adsorbed (mg g^{-1}) at time t, and at equilibrium, respectively, k_1 is the rate constant of pseudo-first-order equation (min^{-1}).

3.0 RESULTS AND DISCUSSION

3.1 Scanning Electron Micrographs (SEM) Analysis

The surface morphology and surface texture of the Raw Materials, hybrid adsorbent before and after the adsorption process was examined by SEM analysis, and the result is depicted in Figure 3.1. Figure 3.1(a) shows the SEM image of the raw Moringa seed husk. The image revealed various pores on the surface of the sample studied which indicated a good possibility of metal ions to be absorbed. The SEM image in Figure 3.1(b) shows the image of Raw Neem leaves The SEM image in Figure 3.1(c) Shows the image of hybrid activated carbon produced from Moringa Seed Husk and Neem Leaves, it clearly revealed that the pores earlier seen on the raw Moringa seed husk and Neem leaves has drastically increased as a result of pyrolysis, on the other hand Figure 3.1(d) shows the image of the hybrid adsorbent after adsorption and it can be clearly seen the pores has been covered to adsorption.

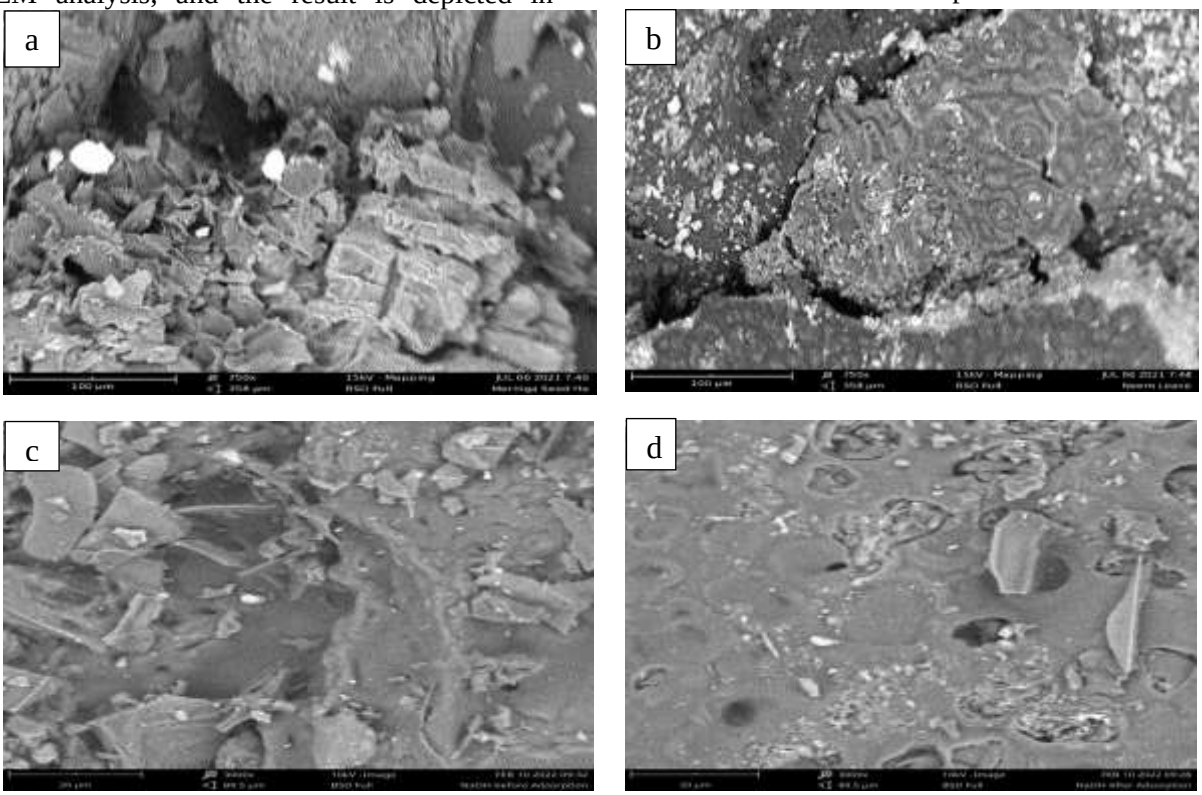

Figure 3.1: SEM images (a) Raw Moringa seed Husk (b) Raw Neem Leaves (c) NEMO Adsorbent before Adsorption (d) NEMO Adsorbent after Adsorption

3.2 Energy Dispersive X-ray Spectroscopy (EDX) Analysis

EDX analysis of the samples are given in Figure 3.2(a) Shows the result of the elemental composition of Raw Moringa Seed Husk, Figure 3.2(b) Shows EDX Analysis of Raw Neem Leaves, Figure 3.2(c) Shows the image of NEMO Adsorbent before Adsorption, and Figure 3.2(d) Shows the image of NEMO Adsorbent after Adsorption. It is clearly seen from the results that the raw neem leaf samples consist of different ratios of carbon, potassium, strontium and calcium. EDX analysis revealed the presence of phosphorus, which showed good adsorption properties, especially for neem leaf. This analysis also showed the presence of trace amounts of Ca, Mg, Br, Fe and Si.

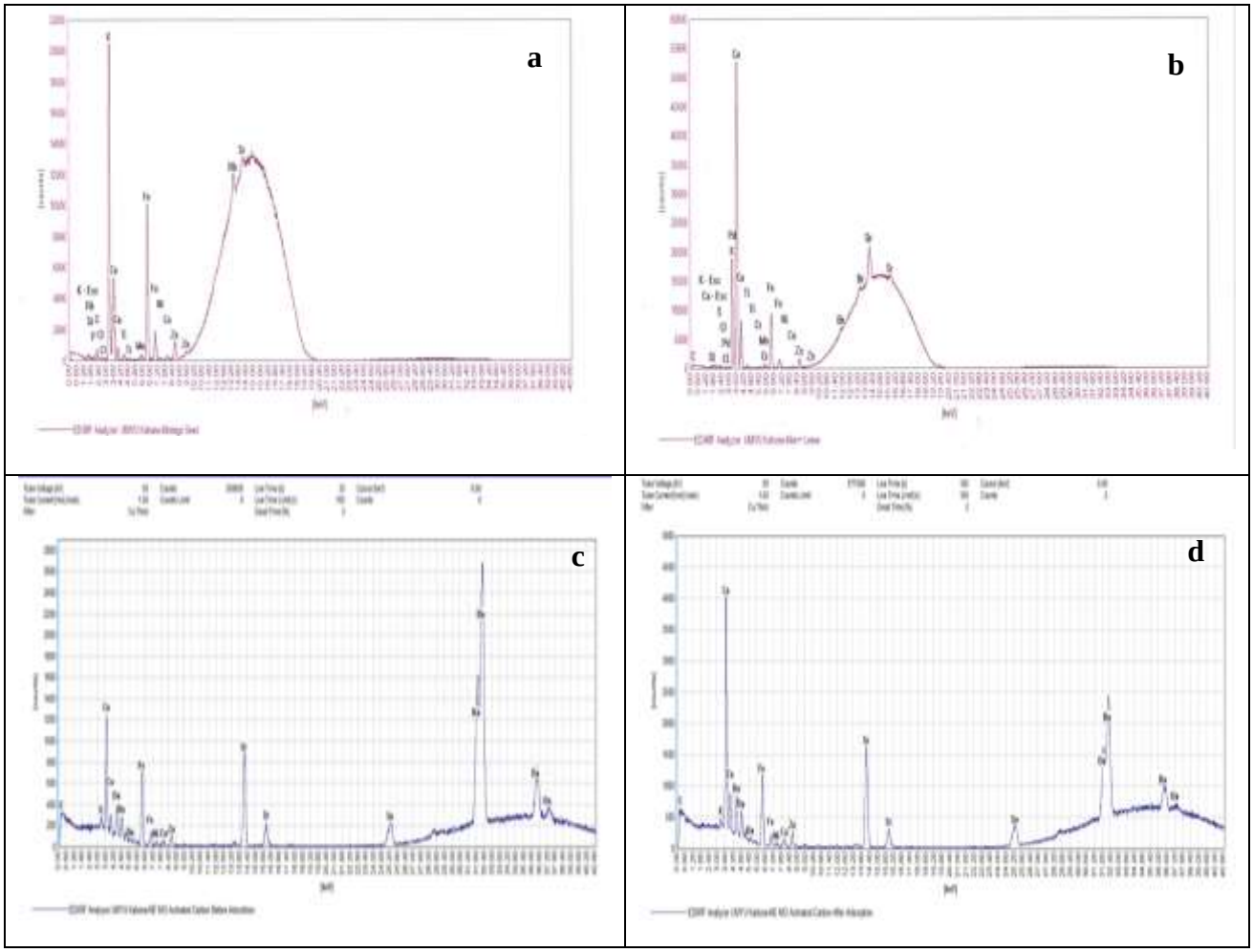

Figure 3.2: EDX Analysis (a) Raw Moringa seed Husk (b) Raw Neem Leaves (c) NEMO Adsorbent before Adsorption (d) NEMO Adsorbent after Adsorption

SEM demonstrates increased surface porosity after activation, while EDS confirms dye capture. Together, these analyses prove that activation enhances adsorption capacity by increasing the number and effectiveness of adsorption sites.

3.3 Fourier Transform Infra-Red Spectroscopy

The functional groups of the samples were determined using Fourier transform-infrared spectroscopy (SHIMADZU-FTIR-8400S). Figure 3.3 shows the functional groups present in the Moringa oleifera seed husk and that of the Neem leave. Neem leaves contain bioactive

compounds like tannins, flavonoids, and polyphenols. FTIR analysis of Neem Leaves shows key functional groups such as: Hydroxyl (–OH) groups (3200–3600 cm^{-1}) enable hydrogen bonding with dye molecules. Carboxyl (–COOH) groups (1700–1750 cm^{-1}) facilitate ion-exchange with cationic dyes. C–O stretching (1000–1200 cm^{-1}) from phenolic compounds enhances chemical interactions. Alkyl C–H groups (2850–2950 cm^{-1}) promote hydrophobic interactions with nonpolar dyes and for Moringa Seed Husk is rich in lignocellulosic material and contains Hydroxyl (–OH) groups (3200–3600 cm^{-1}) for hydrogen bonding, Carboxyl (–COOH**)** (1700 cm^{-1}) and carbonyl groups (1600–1650 cm^{-1}) for electrostatic and π-π interactions with dye molecules, C–O stretching (1000–1200 cm^{-1}) and aromatic C–H groups (1400–1500 cm^{-1}), improving adsorption through Van der Waals forces and aromatic stacking. Each of the bands on the FTIR represents a particular functional group which enables adsorption. Alkyl C–H groups (2850–2950 cm^{-1}) promote hydrophobic interactions with nonpolar dyes and for Moringa Seed Husk is rich in lignocellulosic material and contains Hydroxyl (–OH) groups (3200–3600 cm^{-1}) for hydrogen bonding, Carboxyl (–COOH**)** (1700 cm^{-1}) and carbonyl groups (1600–1650 cm^{-1}) for electrostatic and π-π interactions with dye molecules, C–O stretching (1000–1200 cm^{-1}) and aromatic C–H groups (1400–1500 cm^{-1}), improving adsorption through Van der Waals forces and aromatic stacking.

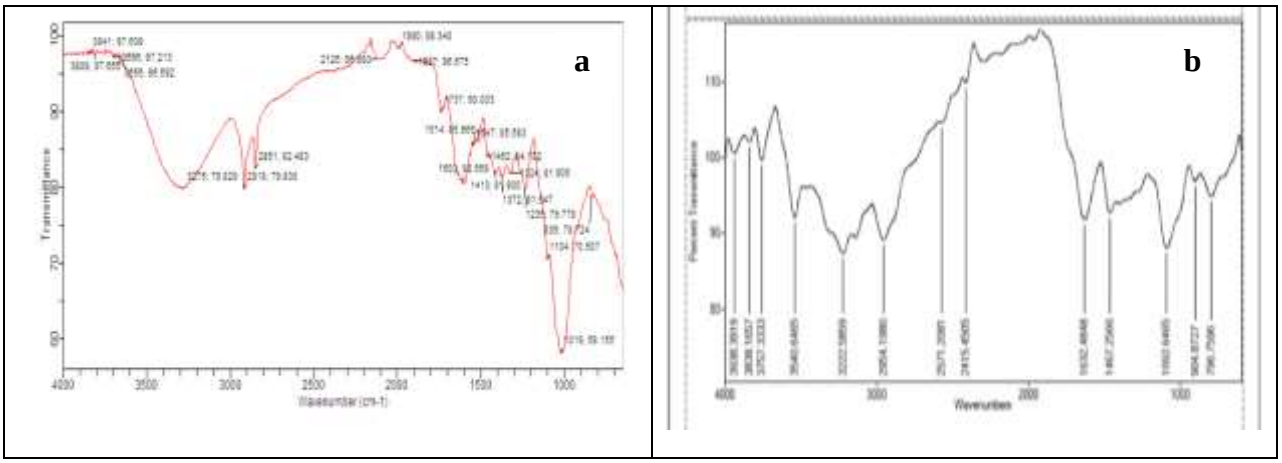

Figure 3.3: (a) Raw Moringa Seed Husk FTIR (b) Raw Neem Leave FTIR

However, from the FTIR spectra shown in Figure 3.4 (a) before and (b) after adsorption, it can be noted that there are new peaks appearing after the adsorption process. The characteristic peaks at 3529 cm^{-1} and 1261 cm^{-1} which may be assigned to Si— O bending vibration and N–H stretching vibrations are only found on adsorbent before adsorption and after adsorption, respectively. In addition, the characteristic peaks at 3427 cm^{-1}, 1881 cm^{-1} and 906 cm^{-1} assigned to —OH stretching vibrations, Si— O bending vibration and aromatic —CH out of plane structure appeared on the adsorbent after the adsorption which may be attributed to the present of contaminants on the adsorbent but are lacking on adsorbent before adsorption. The combination of Neem leaves and Moringa seed husk creates a synergistic effect due to the diversity of functional groups. Both materials offer multiple interaction sites for various dye molecules, enhancing adsorption efficiency through hydrogen bonding, electrostatic interactions, π-π stacking, and hydrophobic forces. This functional diversity makes them a promising, eco-friendly, and cost-effective adsorbent for dye removal

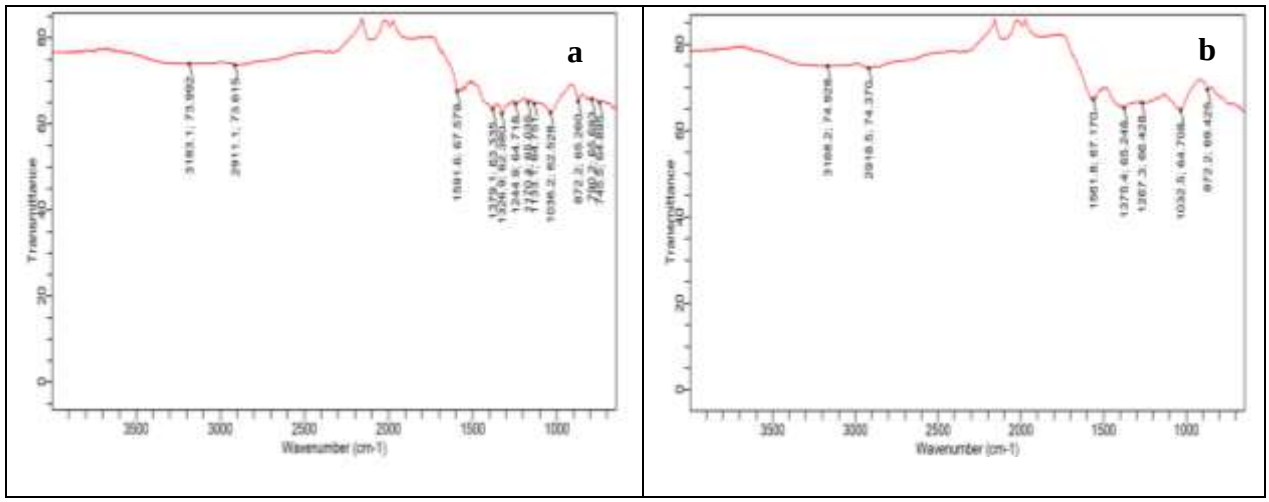

Figure 3.4: (a) NEMO Before Adsorption (b) NEMO after Adsorption

3.4 Effect of Parameters

In this experiment, specific parameter ranges—such as pH, contact time, and temperature—are selected based on practical relevance, system behavior, and prior research findings**.** Practical relevance is considered by choosing ranges like pH 6–8. Similarly, the chosen contact time and temperature match operational conditions found in industrial and environmental processes.

3.4.1 Effect of Dosage

A series of experiments were conducted to determine the effect of adsorbent dosage by varying the adsorbent dosage from 0.1 g to 1.2 g. Measurements were performed by stirring 50 ml of MB solution with an initial concentration of 100 mg/l using a mechanical shaker for about 60 minutes, and the residual dye concentrations were analyzed using UV spectrophotometer. When the adsorbent increases within the range from 0.1g - 0.4g, the adsorption efficiency of methylene blue dye increases significantly, the reason is that the increase of the adsorbent within a certain range provides more active adsorption sites for the adsorption system, and at this time the dosage of the adsorbent is low, and the distance between the active adsorption sites is large. As the amount of adsorbent increased from 0.1 - 0.7 g. The percentage of adsorbed dye increased from 76.5 - 89.2%, and when the amount of adsorbent exceeds 0.7 g, the amount adsorbed decreased. The possible reason for this trend is that the shielding effect was formed around the high concentration of adsorbent, the binding capacity was weakened, the steric hindrance caused by the accumulation of excessive adsorbents between the adsorbents, the available active adsorption points are reduced and the effective surface adsorption or ion exchange effect is also weakened. Increasing the dosage of adsorbent can lead to both the shielding effect, where dense packing and particle aggregation reduce the accessibility of adsorption sites and decrease effective adsorption capacity, and steric hindrance, where physical blockage of adsorption sites and restricted movement of dye molecules reduce adsorption efficiency and slow down the rate of adsorption. Therefore, while higher dosages might initially seem beneficial, they can lead to diminishing returns in adsorption efficiency beyond an optimal point, making it essential to understand these effects for optimizing adsorbent dosage and achieving the best results in dye removal processes.

The decline in adsorption efficiency beyond a certain adsorbent dosage can be attributed to two primary factors: Shielding Effect**:** As the dosage increases, adsorbent particles may become densely packed and aggregate, reducing the accessibility of adsorption sites. This phenomenon has been observed in studies by Wang *et al.* (2010) and Khan *et al.* (2018**).** Steric Hindrance**:** Higher dosages can lead to physical obstruction of adsorption sites and restrict the movement of dye molecules, as evidenced by research conducted by Lee *et al.* (2016) and Zhang *et al.* (2014). Understanding these effects is essential for optimizing

adsorbent dosage to achieve maximum adsorption efficiency. Excessive dosages can result in diminishing returns in adsorption performance, underscoring the need to determine the optimal balance for effective dye removal.

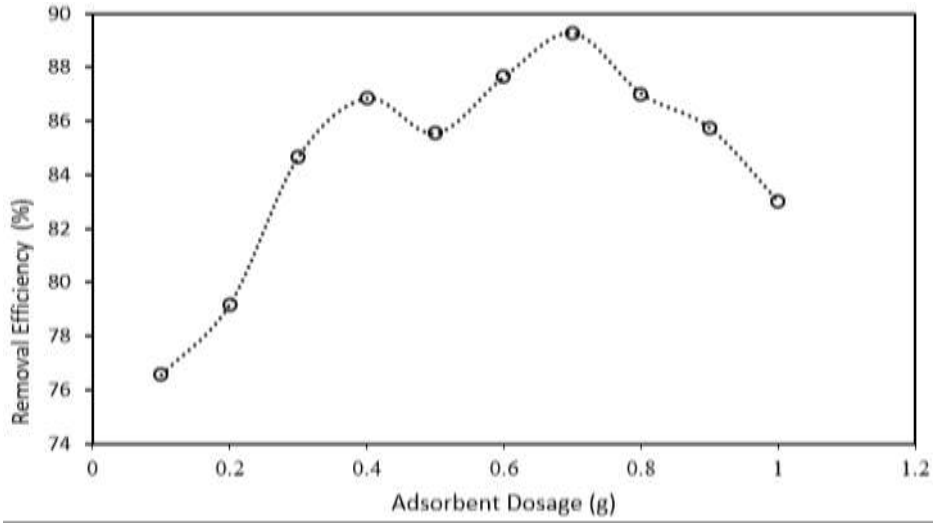

Figure 3.5*:* Effect of Adsorbent Dosage

Figure 3.5 shows the plot between the removal efficiency (%) against dosage (g). it was observed that, the amount of dye adsorbed was varied with varying sorbent mass in the synthetic effluent medium and it decreased with increase in adsorbent mass. The possible reason may be all the active sites were completely exposed and utilized at lower adsorbent dosage in the medium. Each active site will help more methylene blue molecules to gather which was beneficial to the effective surface adsorption or ion exchange between adsorbent and methylene blue. Moreover, we speculate that only part of the active sites was exposed and occupied by MB at higher adsorbent dosage. Hence, the present adsorption studies describe a falling R.E values with respect to the adsorbent mass as depicted.

3.4.2 Effect of Contact Time

At 30 °C, 0.7g adsorbent dose, methylene blue solution (initial concentrations are 100mg/L), within 20 -180 min were studied as shown in Figure 3.6. The removal of dye by adsorption was found to be rapid at the initial period of contact time, and then to became slow with the increase of contact time. The results show that the activated carbon has a faster adsorption rate for methylene blue, and the adsorption rate can reach more than 91% in about 120 minutes. The adsorption of methylene blue mainly occurred on the surface of the adsorbent in the initial stage. The appearance provides a huge surface area with a high probability that the methylene blue dye molecules are in effective contact with the numerous active sites of the adsorbent. After 120 min, the adsorption reached equilibrium, and the adsorption rate and adsorption capacity basically stopped increasing. At this point, most of the active adsorption sites on the surface of the adsorbent are occupied.

The probability of contact with the adsorption site was greatly reduced, the adsorption site can only be found by inward diffusion, and the adsorption process was slowed down. This adsorption model with faster deceleration in the early and late stages was caused by the concentration difference. When the adsorbent was added, the concentration of the adsorption system was large, the driving force for mass transfer was large, and the adsorption rate was fast; as the adsorption progresses, the adsorption concentration difference between the surface area and mass of the adsorbent gradually decreases, and the driving force for mass transfer decreases.

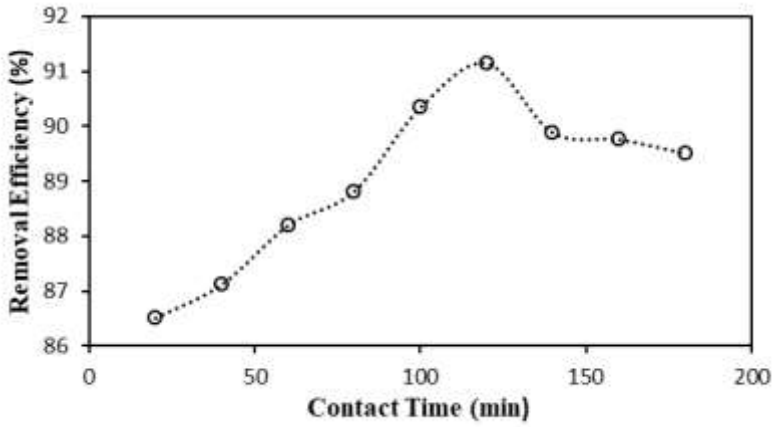

Figure 3.6: Effect of Contact Time

3.4.3 Effect of pH

The amount of dye removal and effect of pH was analyzed over the pH range of 6 to 8. The pH was adjusted by using 0.1N NaOH and 0.1N HCl solutions. From Figure 3.7, it was observed that the solution pH (6 to 8) affected the amount of dye adsorbed in the synthetic effluent medium. The dye sorption behaviour relative to solution pH can be described by several reasons. There are large numbers of active sites on the surface of adsorbent to which the solute uptake can be related. The chemistry of solute in the effluent solution plays an important role in describing the behaviour of its ions. As the pH of the system increases, the number of positively charged sites increases. Subsequently, the negatively charged sites favour the adsorption of dye cations due to electrostatic attraction (Padmavathy *et al.*, 2016), precluding the electrostatic attraction with the MB decreasing the adsorbate uptake. At lower pH, the surface charge may get positively charged, thus making H^+ ions compete effectively with the dye cations causing a decrease in the amount of dye adsorbed (Sowmya *et al.*, 2015)

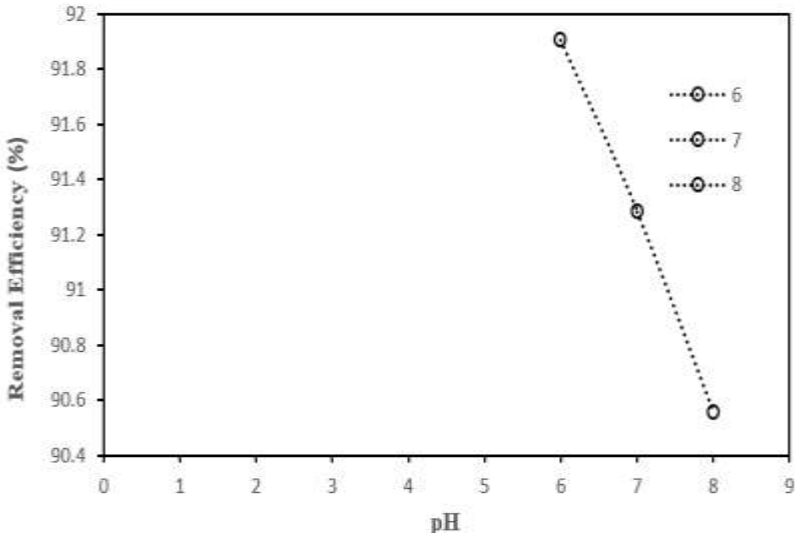

Figure 3.7: Effect of pH

3.4.4 Effect of Temperature

To study the effect of temperature on the adsorption of dye, the experiments were performed at temperatures of 20°C - 60°C. As it was observed in Figure 3.8, the equilibrium adsorption capacity of MB was found to increase with increasing temperature, especially in higher equilibrium concentration, or lower adsorbent dose because of high driving force of adsorption. This fact indicates that the mobility of dye molecules increased with the temperature. The adsorbent shows the endothermic nature of adsorption. Under the same initial concentration conditions, as the temperature increases, the adsorption capacity qe of methylene blue increase slightly.

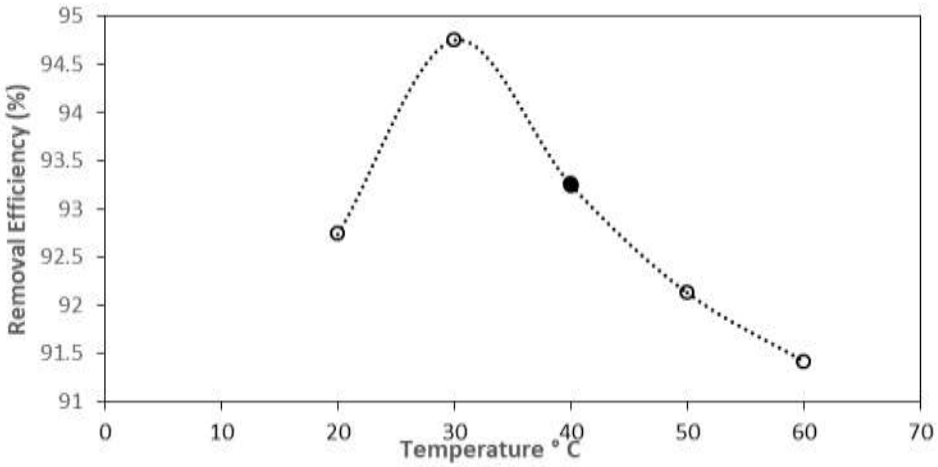

Figure 3.8: Effect of temperature

3.4.5 Effect of Initial Dye Concentration

The effect of initial dye concentration was estimated for every 20 minutes by contacting 0.5 g of the produced adsorbent with 50 ml of MB solutions at different initial concentrations ranging from 100 to 500 mg/L for 180 minutes. Experiments were performed at optimum pH of 6, temperature of 30 °C, 0.7g Dosage and 120 min time. Figure 3.9 shows the plot between amounts of dye adsorbed Qt (mg/g) versus time (min) for initial dye concentration of 100, 200, 300, 400 and 500 mg/L. It was observed that the amount of dye adsorbed Qt (mg/g) increased with respect to an increase in initial dye concentration from 100 to 400 mg/L. During the adsorption process, initially the dye molecules reach to the boundary layer and then they diffused into the porous structure of the adsorbent. The amount of dye adsorbed (mg/g) increased with increase in time and then reaches the equilibrium. The supernatant was analyzed by using UV-Spectrophotometer at 665nm. The effect of initial dye concentration on MB removal percentage and adsorption capacity of adsorbent were determined from the results.

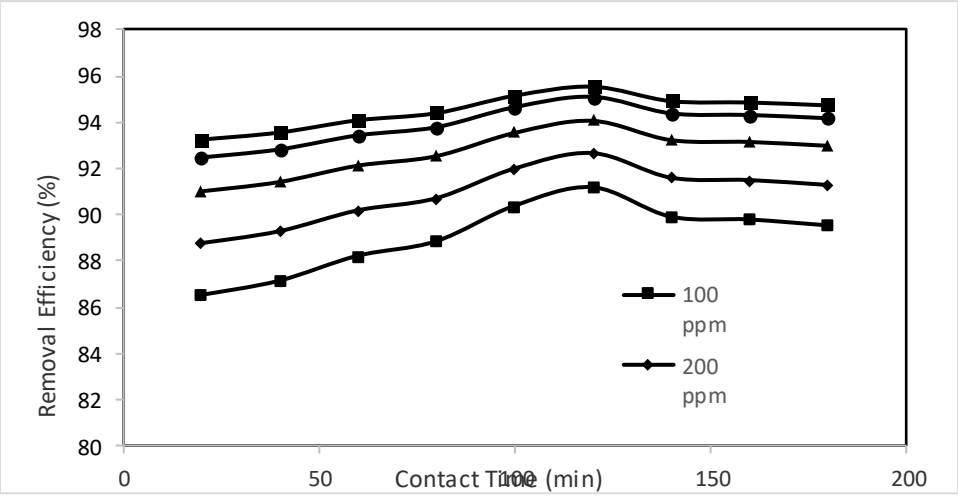

Figure 3.9: Effect of initial dye concentration

3.5 Isotherms and Kinetics Studies

3.5.1 Isotherms Models

An adsorption isotherm is an important curve describing the phenomenon governing the retention (or release) or mobility of a substance from the aqueous porous media or aquatic environments to a solid-phase at a constant temperature and pH. In this study, three adsorption isotherm models (Langmuir, Freundlich and Temkin) were fitted to experimental equilibrium data for Methylene blue dye. The modeled adsorption isotherm plot for Methylene blue dye is shown in Figure .3.10 Correlation coefficient (R^2) has been found to be 0.9862, 0.9571 and 0.9273 Langmuir, Freundlich and Temkin respectively. The R^2 which is close to unity indicates strong correlation. Hence, from this research, the experimental results indicated the adsorption of MBD on to NEMO AC follows Langmuir isotherm model data as the R^2 was close to unity compared to Freundlich and Temkin isotherms.

The Langmuir model better fit than the Freundlich and Temkin models for the adsorption of process due to its effective description of monolayer coverage and finite, uniform adsorption sites. This model accurately predicts the saturation behavior observed with these adsorbents, which exhibit well-defined adsorption capacities. In contrast, the Freundlich model's assumption of heterogeneous sites and the Temkin model's focus on adsorbate interactions may not adequately represent the adsorption behavior of these natural materials.

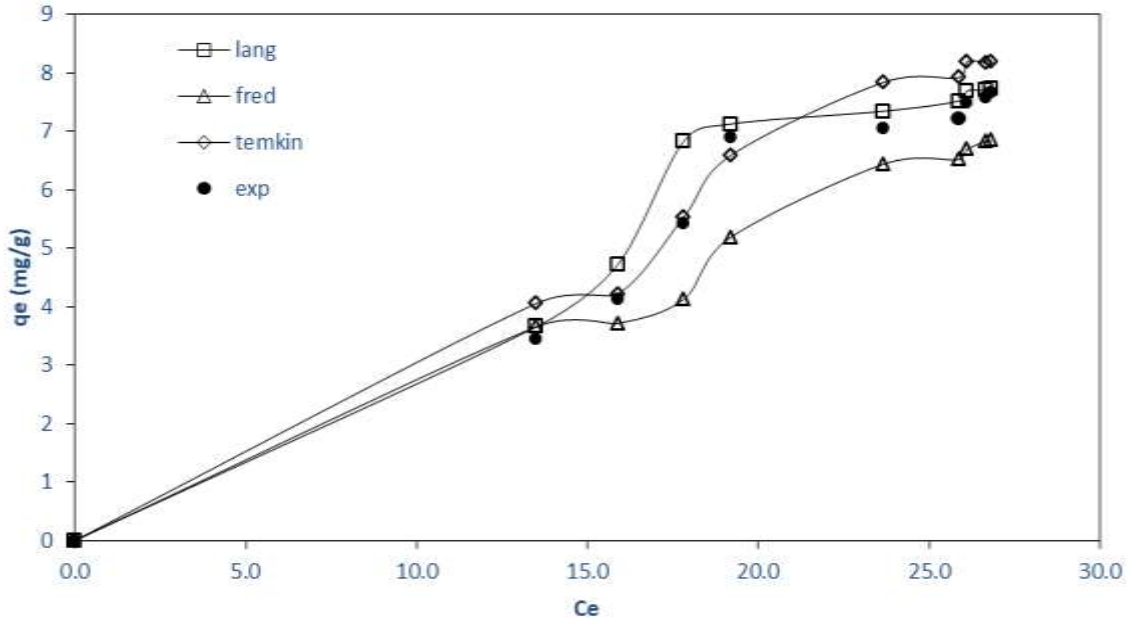

Fig. 3.10: Langmuir, Freundlich and Temkin isotherms Model

3.5.2 Adsorption Kinetics

The analysis of the adsorption uptake of Methylene blue from waste water at different time intervals was conducted in order to test the kinetics models of the system. The data were fitted to pseudo-first-order and pseudo- second-order models, to obtain the constant parameters. The conformity between experimental data and the model predicted values was expressed by correlation coefficient (R^2), and further understanding of the effect of time on the adsorption process was obtained from the kinetic treatment of data using pseudo-first-order and pseudo-second-order models. Using the regression correlation (R^2) value, the pseudo second-order model better described the adsorption process than pseudo-first-order. In addition, the calculated qe, from this pseudo-second-order agrees with the one obtained experimentally. This suitability of pseudo-second-order indicates that chemical interaction was involved in the adsorption process of MB on to the activated carbon.

When the pseudo-second-order model fits well with adsorption data, it typically indicates a chemisorption process, characterized by the formation of strong chemical bonds between the adsorbate (methylene blue) and the adsorbent (e.g., Moringa seed husk or neem leaves). This suggests that dye molecules interact with specific functional groups on the adsorbent through chemical reactions or strong electrostatic interactions. The model also implies that the rate-limiting step is related to these bond formations, making the adsorption rate dependent on the availability of active sites and the efficiency of bond formation.

Studies involving Moringa seed husk and neem leaves frequently demonstrate a good fit for the pseudo-second-order model, supporting the chemisorption mechanism due to the presence of functional groups like hydroxyl, carboxyl, and phenolic groups that engage in strong interactions with dye molecules (Rao *et al.,* 2012; Singh *et al.,* 2014).

The prevalence of the pseudo-second-order model in various studies, such as those **by** Ho and McKay (1998) and Zhou *et al.* (2017)**,** highlights its suitability for describing adsorption processes where strong interactions between adsorbent and adsorbate are involved. These studies commonly find that materials with high surface reactivity or functional groups conducive to chemical bonding (like those found in Moringa seed husk and neem leaves) align well with the pseudo-second-order kinetics.

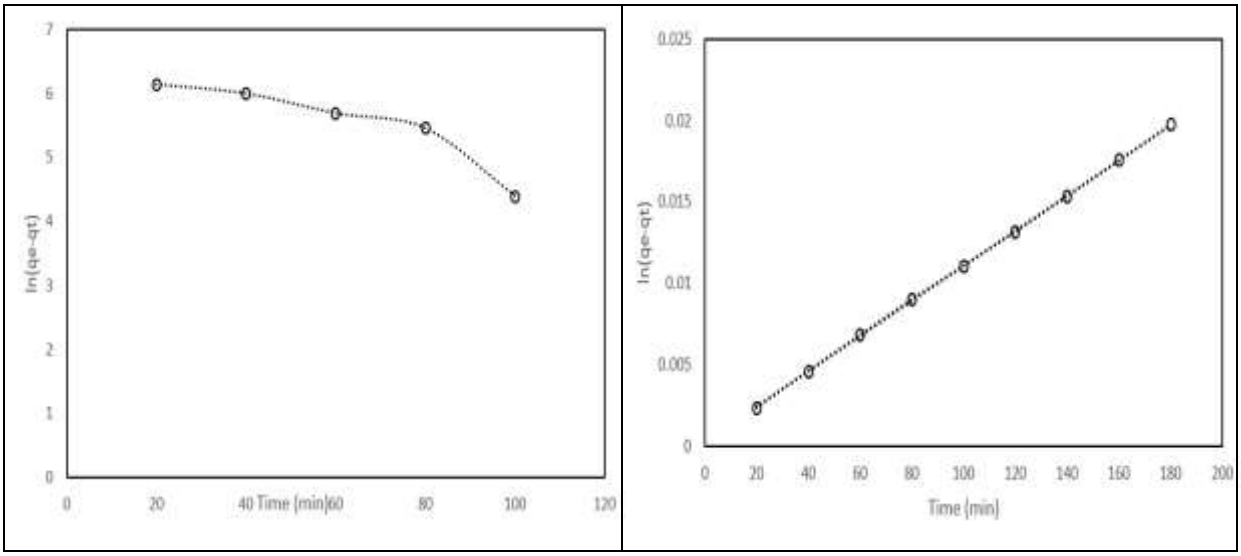

Figure 3.11: (a) Pseudo first order kinetic model (b)Pseudo second order kinetic model

4.0 CONCLUSION

A composite activated carbon, NEMO AC was developed from the biochar of the two precursors and was utilized as a low-cost adsorbent for the removal of MB dye from aqueous solution. The materials were characterized using SEM, FTIR and EDX at its raw stage, before activation and after adsorption. However, the material showed an enhanced surface morphology elemental composition and functional group which aids its adsorption capacity. The effect of kinetic parameters revealed, that the optimum equilibrium conditions in the experiment were found to be pH of 6, temperature of 30 °C, 0.7g dosage, 120 min contact time and the initial dye concentration of 400 mg/l. The experimental data were fitted to adsorption isotherms and kinetics Models, the adsorption followed the Langmuir Model, while the Kinetic studies followed pseudo-second-order kinetic model showing the adsorption was controlled by chemisorption process. Natural adsorbents like Neem and Moringa face challenges in regeneration**,** as they are difficult to reuse after adsorption, necessitating research into simple and low-cost regeneration methods to improve their long-term viability

REFERENCES

Al-ghouti, M. A., & Da'ana, D. A. (2020). Guidelines for the use and interpretation of adsorption isotherm models: A review. Journal of Hazardous Materials, 393, 122383. https://doi.org/10.1016/j.jhazmat.2020.122383

Bagheri, A., Abu-Danso, E., & Iqbal, J. (2020). Modified biochar from Moringa seed powder for the removal of diclofenac from aqueous solution. Environmental Science and Pollution Research, 27(7), 7318-7327. https://doi.org/10.1007/s11356-019-06844-x

Bello, M. O., Abdus-Salam, N., Adekola, F. A., & Pal, U. (2021). Isotherm and kinetic studies of adsorption of methylene blue using activated carbon from ackee apple pods. Chemical Data Collections, 31, 100607. https://doi.org/10.1016/j.cdc.2020.100607

Bello, A. A. O., & Adegoke, I. A. G. (2015). Competitive adsorption of dye species from aqueous solution onto melon husk in single and ternary dye systems. International Journal of Environmental Science and Technology, 12(3), 939–950. https://doi.org/10.1007/s13762-013-0469-8

Bello, O. S., Bello, I. A., & Adegoke, K. A. (2013). Adsorption of dyes using different types of sand: A review. Research Journal of Chemical Sciences, 3(5), 117–129.

Das, R., Mukherjee, A., Sinha, I., Roy, K., & Dutta, B. K. (2020). Synthesis of potential bio-adsorbent from Indian neem leaves (Azadirachta indica) and its optimization for malachite green dye removal from industrial wastes

using response surface methodology: Kinetics, isotherms, and thermodynamic studies. Applied Water Science, 10(5), 1–18. https://doi.org/10.1007/s13201-020-01184-5

Foo, K. Y., & Hameed, B. H. (2010). Insights into the modeling of adsorption isotherm systems. Chemical Engineering Journal, 156(1), 2–10. https://doi.org/10.1016/j.cej.2009.09.013

Glocheux, Y., Albadarin, A. B., Galán, J., Oyedoh, E., Mangwandi, C., Gérente, C., Allen, S. J., & Walker, G. M. (2014). Adsorption study using optimized 3D organized mesoporous silica coated with Fe and Al oxides for specific As (III) and As (V) removal from contaminated synthetic groundwater. Microporous and Mesoporous Materials, 198, 101–114. https://doi.org/10.1016/j.micromeso.2014.07.020

Gopalakrishnan, L., Doriya, K., & Kumar, D. S. (2016). Moringa oleifera: A review on nutritive importance and its medicinal application. Food Science and Human Wellness, 5(2), 49–56. https://doi.org/10.1016/j.fshw.2016.04.001.

Jami, M. S., & Ahmad, M. M. (2020). Elemental and chemical composition of Moringa oleifera husk. Journal of Chemical Engineering and Industrial Biotechnology, 5(1). https://doi.org/10.15282/jceib.v5i1.3897

Padmavathy, K. S., Madhu, G., & Haseena, P. V. (2016). A study on effects of pH, adsorbent dosage, time, initial concentration and adsorption isotherm study for the removal of hexavalent chromium (Cr (VI)) from wastewater by magnetite nanoparticles. Procedia Technology, 24, 585–594. https://doi.org/10.1016/j.protcy.2016.05.127

Periodicals, W. (2012). Is scanning electron microscopy/energy dispersive X-ray spectrometry (SEM/EDS) quantitative? Scanning Journal of Microscopy, 34(1), 1–28. https://doi.org/10.1002/sca.21041

Onundi, Y. B., Mamun, A. A., Khatib, M. F., & Ahmed, Y. M. (2010). Adsorption of copper, nickel, and lead ions from synthetic semiconductor industrial wastewater by palm shell activated carbon. International Journal of Environmental Science and Technology, 7(4), 751–758.

Seow, T. W., & Lim, C. K. (2016). Removal of dye by adsorption: A review. International Journal of Applied Environmental Sciences, 11(4), 2675–2679.

Sharma, N., Tiwari, D. P., & Singh, S. K. (2012). Decolourisation of synthetic dyes by agricultural waste: A review. International Journal of Environmental Sciences, 3(2), 1–10.

Singla, S., Kaushal, J., & Mahajan, P. (2017). Removal of dyes from wastewater by plant waste. In Materials Science and Engineering Technology (Vol. 11, pp. 228–239).

Sowmya, S. R., Madhu, G. M., Sankannavar, R., & Yerragolla, S. (n.d.). Adsorption using chitosan and nano zerovalent iron composite material for sustainable water treatment.

Tiwari, P. N. (2002). Removal of basic dye from industrial wastewater by adsorption: Effect of initial dye concentration and contact time. Journal of Environmental Protection, 1(0).

Wang, J., & Guo, X. (2020a). Adsorption isotherm models: Classification, physical meaning, application, and solving method. Chemosphere, 249, 127279. https://doi.org/10.1016/j.chemosphere.2020.127279

Wang, J., & Guo, X. (2020b). Adsorption kinetic models: Physical meanings, applications, and solving methods. Journal of Hazardous Materials, 390, 122156. https://doi.org/10.1016/j.jhazmat.2020.122156